Journal of Organometallic Chemistry 694 (2009) 3395–3400

Contents lists available at ScienceDirect

Journal of Organometallic Chemistry

journal homepage: www.elsevier.com/locate/jorganchem

Synthesis and reactivity of the five-coordinate $\{Fe(NO)_2\}^9$ [(TMEDA)Fe(NO)$_2$I]

Chien-Hong Chen [a,b,*], Yi-Chieh Ho [a], Gene-Hsiang Lee [c]

[a] School of Applied Chemistry, Chung Shan Medical University, Taichung City 40201, Taiwan
[b] Department of Medical Research, Chung Shan Medical University Hospital, Taichung City, Taiwan
[c] Instrumentation Center, National Taiwan University, Taipei, Taiwan

ARTICLE INFO

Article history:
Received 2 June 2009
Received in revised form 30 June 2009
Accepted 30 June 2009
Available online 4 July 2009

Keywords:
DNICs
Protein-bound DNICs
Low-molecular-weight DNICs

ABSTRACT

The reaction of [Fe(μ-I)(NO)$_2$]$_2$ and TMEDA in a 1:2 molar ratio in THF affords the neutral five-coordinate DNIC [(TMEDA)Fe(NO)$_2$I] (**1**). The single-crystal X-ray structure shows that the geometry of iron center of complex **1** is best described as a distorted trigonal bipyramidal with two nitrosyl groups positioned in the equatorial plane. The EPR spectrum of complex **1** displays the six-line signal with $g = 2.031$ ($a_I = 37.6$ G) at 298 K. The coincident g values of EPR among complex **1**, protein-bound DNICs and low-molecular-weight DNICs implicate that the five-coordinate DNICs may exist in biological system. The interconversion between complex **1** and [(TMEDA)Fe(NO)$_2$] (**2**) reveals that the $\{Fe(NO)_2\}^9$ DNICs containing [amine, amine] ligation mode could be stabilized by the five-coordinated geometry while the $\{Fe(NO)_2\}^{10}$ DNICs containing [amine, amine] ligation mode favors the four coordination sphere. In addition, the transformation from complex **1** to [Fe(NO)$_2$(C$_3$H$_3$N$_2$)]$_4$ (**3**), [Fe(μ-SPh)(NO)$_2$]$_2$ (**4**), [PPh$_4$][(PhS)$_2$Fe(NO)$_2$] (**5**) and [Na-18-crown-6-ether][(C$_3$H$_3$N$_2$)$_2$Fe(NO)$_2$] (**6**), respectively, in the presence of thiolates or imidazolates indicates that complex **1** could be employed as the precursor for the syntheses of the DNICs containing the [N,N]/[N,S]/[S,S] different ligations.

1. Introduction

Nitric oxide (NO) first characterized by Priestley in 1772 is the simplest thermally paramagnetic molecule [1]. In addition to the curiosity in the physical and chemical properties for chemists, nitric oxide is also of great interest in the physiological and biological functions in living organisms, including principal neurotransmitter mediating erectile function [2], a critical endogenous regulator of blood flow and thrombosis [3,4], a major path physiological mediator of inflammation and host defense [5]. Dinitrosyl iron complexes (DNICs), the endogenous nitroso compounds as S-nitrosothiols (RSNO), provide the stabilization/storage/transport of NO molecules in biological system [6–9]. DNICs are classified into protein-bound DNICs serving as the storage of NO or $\{Fe(NO)_2\}$ moiety and low-molecular-weight DNICs (LMW DNICs) acting as the donor of NO or $\{Fe(NO)_2\}$ moiety [10–13]. In vitro/vivo, both protein-bound DNICs and LMW DNICs are possibly identified and characterized by their distinctive electron paramagnetic resonance (EPR) signals at $g = 2.03$ [14–17]. In spite of the major thiol components of cellular DNICs composed of cysteine and glutathione in vivo [18], the DNICs ligated by cysteinate, histidine, deprotonated imidazole, and tyrosinate were found and proposed in enzymology based on EPR spectra [11,19–24]. Recently, the protein-bound DNIC with one sulfur atom of the glutathione and one oxygen atom of the tyrosine bound to the $\{Fe(NO)_2\}$ core has been well characterized by X-ray diffraction study via the addition of a dinitrosyldiglutathionyl iron complex into human glutathione transferase P1-1 in vitro/vivo [21]. Although the protein-bound DNIC containing [S,O] ligation mode was well characterized by X-ray diffraction, it is still difficult to extract and isolate DNICs for the biological study. The difficulty has prompted efforts in syntheses of suitable DNICs for the spectroscopic references and the study of potential NO delivery systems. Li et al. and Ford et al. have reported the X-ray structures of the $\{Fe(NO)_2\}^9$ and $\{Fe(NO)_2\}^{10}$ DNICs with the [N,N] ligation mode, respectively [25,26]. Recently, numbers of molecular models of LMW DNICs containing various ligation modes [S,S]/[S,O]/[S,N]/[N,N] were synthesized by Liaw et al. [27–33]. Based on the study of these reported DNICs, the characterization of the $\{Fe(NO)_2\}^9$ DNICs containing various coordinated ligands (thiolate, imidazole, amide, carboxylate, and imidazolate) has been made possible via the combination of EPR (pattern) and IR ν_{NO} spectra (the separation of NO stretching frequencies). The reactivity study of DNICs demonstrates the interconversion among Roussin's red ester (RRE), anion $\{Fe(NO)_2\}^9$ DNICs with [S,S]/[S,O]/[S,N]/[N,N] coordination modes, cationic $\{Fe(NO)_2\}^9$ DNICs and neutral $\{Fe(NO)_2\}^{10}$ DNICs with [N,N] coordination mode. In addition, the study of DNICs with [S,S] ligation

* Corresponding author. Address: School of Applied Chemistry, Chung Shan Medical University, Taichung City 40201, Taiwan.
E-mail address: cchwind@csmu.edu.tw (C.-H. Chen).

0022-328X/$ - see front matter © 2009 Elsevier B.V. All rights reserved.
doi:10.1016/j.jorganchem.2009.06.040

mode also reveals that the stability and the NO-releasing ability of DNICs is regulated by the coordinated thiolate ligands. Furthermore, the photolysis reactions of two similar DNICs, discriminated by the existence of the well-designed [N–H...S] intramolecular interaction, suggest that the [N–H...S] intramolecular interaction induces the more efficient NO-releasing ability [34]. Although DNICs are well-known as the four-coordinate species, the nonclassical six-coordinate $\{Fe(NO)_2\}^9$ DNICs ($[(1\text{-Melm})_2(\eta^2\text{-ONO})\text{-}Fe(NO)_2]$) with chelating nitrito ligand has been characterized and the further reactivity study led to the conclusion that the nonclassical six-coordinate nitrite-containing $\{Fe(NO)_2\}^9$ DNICs serving as the active center to trigger the transformation of nitrite into nitric oxide [35]. To our knowledge, only one example of DNICs, $[(6\text{-}Me_3\text{-TPA})Fe(NO)_2][ClO_4]$ containing five-coordinate geometry has been reported [36]. The results reported here are the synthesis, characterization and reactivity of the neutral five-coordinate $\{Fe(NO)_2\}^9$ DNICs [(TMEDA)$Fe(NO)_2$I] (**1**).

2. Experimental

Manipulations, reactions, and transfers were conducted under nitrogen according to Schlenk techniques or in a glovebox (nitrogen gas). Solvents were distilled under nitrogen from appropriate drying agents (diethyl ether from CaH_2; acetonitrile from CaH_2–P_2O_5; methylene chloride from P_2O_5; hexane and tetrahydrofuran (THF) from sodium benzophenone) and stored in dried, N_2-filled flasks over 4 Å molecular sieves. Nitrogen was purged through these solvents before use. Solvent was transferred to the reaction vessel via stainless cannula under positive pressure of N_2. The reagents tetraphenylphosphonium bromide ([PPh_4][Br]) (Fluka), iron pentacarbonyl (Strem), *N,N,N′,N′*-tetramethylethylenediamine(TMEDA), sodium imidazole, bis(cyclopentadienyl)cobalt(II), 18-crown-6-ether, benzenethiol (Aldrich–Sigma) were used as received. $[Fe(\mu\text{-}I)(NO)_2]_2$ [37] and [(TMEDA)$Fe(NO)_2$] [31] have been prepared according to the literature procedure. Infrared spectra of the nitrosyl ν(NO) stretching frequencies were recorded on a Jasco FT/IR-4100 spectrophotometer with sealed solution cells (0.1 mm) and KBr windows. UV/vis spectra were recorded on a GBC Cintra 101. Analyses of carbon, hydrogen, and nitrogen were obtained with a CHN analyzer (Heraeus).

2.1. Preparation of [(TMEDA)$Fe(NO)_2$I] (**1**)

To a stirred solution of $[Fe(\mu\text{-}I)(NO)_2]_2$ (0.486 g, 1 mmol) in THF (10 mL) was added TMEDA (305 μL, 2 mmol) dropwise under N_2 at ambient temperature. After being stirred for 3 h, the reaction solution was filtered through Celite to give the yellow-green filtrate. The volume of the filtrate was reduced to 3 mL under vacuum and then hexane (20 mL) was added to precipitate the brown solid [(TMEDA)$Fe(NO)_2$I] (**1**) (0.58 g, 81%). Diffusion of hexane into the THF solution of complex **1** at −15 °C led to red-brown crystals suitable for single-crystal X-ray diffraction. IR(ν_{NO}): 1770 (s), 1715 (vs) cm^{-1} (THF); 1775 (s), 1717 (vs) cm^{-1} (CH_3CN); 1773 (s), 1719 (vs) cm^{-1} (diethyl ether). Absorption spectrum (THF) [λ_{max}, nm (ε, $M^{-1}\,cm^{-1}$)]: 312 (13 439). Anal. Calc. for $C_6H_{16}FeIN_4O_2$: C, 20.08; H, 4.49; N, 15.61. Found: C, 20.12; H, 5.01; N, 15.23%.

2.2. Reaction of complex 1 with Cp_2Co

Complex **1** (0.072 g, 0.2 mmol) and Cp_2Co (0.038 g, 0.2 mmol) were dissolved in THF (6 mL) and stirred under nitrogen at ambient temperature. After being stirred for 1.5 h, the reaction solution was filtrated through Celite to remove the insoluble solid. The light green filtrate was monitored by FTIR. The IR ν_{NO} spectrum of the filtrate solution showing absorption bands at 1698 (s), 1644 (s) cm^{-1} was assigned to the formation of the neutral $\{Fe(NO)_2\}^{10}$ [(TMEDA)$Fe(NO)_2$] (**2**) [31]. After the filtrate was dried under vacuum, the green solid washed with hexane twice affording 0.038 g of complex **2** (yield 81.2%).

2.3. Reaction of complex 2 with I_2

To the 50 mL Schlenk flask containing 10 mL THF solution of complex **2** (0.232 g, 1 mmol) was added 5 mL THF solution of I_2 (0.127 g, 0.5 mmol) dropwise by a cannula under positive N_2 pressure at ambient temperature. When the reaction mixture was stirred for 1 h, the reaction mixture was monitored by FTIR. The IR ν_{NO} spectrum of the reaction solution showing absorption bands at 1770 (s), 1715 (vs) cm^{-1} was assigned to the reformation of complex **1**. After the yellow-green solution was filtered through Celite, the filtrate was concentrated to 3 mL under vacuum and hexane (30 mL) was added to precipitate the brown solid complex **1** (0.297 g, 83.1%).

2.4. Reaction of complex **1**, 18-crown-6-ether, and sodium imidazole

Complex **1** (0.287 g, 0.8 mmol), 18-crown-6-ether (0.211 g, 0.8 mmol), and sodium imidazole ([Na][$C_3H_3N_2$]) (0.072 g, 0.8 mmol) were dissolved in CH_3CN (8 mL) and stirred for 3 days under nitrogen at ambient temperature. A brown solution accompanied by a light brown solid was formed. The mother-liquor was removed under a positive pressure of N_2 and the residue brown solid was washed with CH_3CN three times. The brown solid was dried under vacuum and then redissolved in 10 mL THF. The IR spectrum showing ν_{NO} stretching frequencies at 1800 (m), 1736 (s) cm^{-1} (THF) indicated the formation of the known cyclic tetranuclear dinitrosyl iron complex $[Fe(NO)_2(C_3H_3N_2)]_4$ (**3**)[25]. The solution was dried under vacuum and diethyl ether was added to redissolve the brown solid. After the red-brown diethyl diether solution was filtered through Celite, the red-brown filtrate was dried under vacuum leading to the brown solid of complex **3** (yield 0.107 g, 72.7%).

2.5. Reaction of complex 1 and [PPh_4][$(PhS)_2Fe(NO)_2$] (or reaction of complex **1** and [PPh_4][SPh])

The 8 mL THF solution of complex **1** (0.144 g, 0.4 mmol) was added into the 20 mL Schlenk tube containing [PPh_4][$(PhS)_2$-$Fe(NO)_2$] (0.269 g, 0.4 mmol) (or [PPh_4][SPh] (0.179 g, 0.4 mmol)) via a cannula under positive N_2 pressure. The reaction solution was stirred for 2 h under N_2 at ambient temperature. The reaction solution was monitored with FTIR. The IR spectrum showing ν_{NO} stretching frequencies at 1814 (w), 1783 (s), 1756 (s) cm^{-1} (THF) was assigned to the formation of the known dinuclear dinitrosyl iron complex $[Fe(\mu\text{-SPh})(NO)_2]_2$ (**4**) [38]. The reaction solution was dried under vacuum and then 20 mL diethyl ether was added to redissolved the brown solid. After being stirred for 10 min, the reaction mixture was filtered through Celite to separate the insoluble solid. The red-brown filtrate was dried under vacuum leading to the brown solid of complex **4** (yield 0.123 g, 68.4%; [PPh_4][SPh]: yield 0.055 g, 61.6%).

2.6. Reaction of complex 1 and 2 equiv. of [PPh_4][SPh]

The 8 mL THF solution of complex **1** (0.144 g, 0.4 mmol) was added into the 20 mL Schlenk tube containing [PPh_4][SPh] (0.358 g, 0.8 mmol) via a cannula under positive N_2 pressure. The reaction solution was stirred overnight under N_2 at ambient temperature. The reaction solution was monitored with FTIR. The IR spectrum showing ν_{NO} stretching frequencies at 1737 (s), 1693 (s) cm^{-1} (THF) was assigned to the formation of the known

complex $[PPh_4][(PhS)_2Fe(NO)_2]$ (**5**) [28]. The reaction mixture was filtered through Celite to separate the insoluble solid. The filtrate was concentrated under vacuum and then hexane was added to the filtrate to precipitate the brown solid **5** (yield 0.162 g, 60.4%).

2.7. Reaction of complex 1 and 2 equiv. of [Na-18-crown-6-ether][$C_3H_3N_2$]

The 8 mL THF solution of complex **1** (0.144 g, 0.4 mmol) was added into the 20 mL Schlenk tube containing 18-crown-6-ether (0.211 g, 0.8 mmol) and sodium imidazole ($[Na][C_3H_3N_2]$) (0.072 g, 0.8 mmol)) via a cannula under positive N_2 pressure. The reaction solution was stirred overnight under N_2 at ambient temperature. The reaction solution was monitored with FTIR. The IR spectrum showing ν_{NO} stretching frequencies at 1774 (s), 1712 (s) cm^{-1} (THF) was assigned to the formation of the known complex [Na-18-crown-6-ether][$(C_3H_3N_2)_2Fe(NO)_2$] (**6**) [33]. The reaction mixture was filtered through Celite to separate the insoluble solid. The filtrate was concentrated under vacuum and then hexane was added to the filtrate to precipitate the brown solid **6** (yield 0.140 g, 65.3%).

2.8. Reaction of complex 3 and [Na-18-crown-6-ether][$C_3H_3N_2$]

The 5 mL THF solution of complex **3** (0.073 g, 0.1 mmol) was added into the 20 mL Schlenk tube containing 18-crown-6-ether (0.106 g, 0.4 mmol), and sodium imidazole ($[Na][C_3H_3N_2]$) (0.036 g, 0.4 mmol) via cannula under positive N_2 pressure. The reaction solution was stirred overnight under N_2 at ambient temperature. The reaction solution was monitored with FTIR. The IR spectrum showing ν_{NO} stretching frequencies at 1774 (s), 1712 (s) cm^{-1} (THF) was assigned to the formation of the known complex [Na-18-crown-6-ether][$(C_3H_3N_2)_2Fe(NO)_2$] (**6**). The reaction mixture was filtered through Celite to separate the insoluble solid. The filtrate was concentrated under vacuum and then hexane was added to the filtrate to precipitate the brown solid **6** (yield 0.111 g, 51.5%).

2.9. Reaction of complex 3 and [PPh_4][SPh]

The 5 mL CH_3CN solution of [PPh_4][SPh] (0.179 g, 0.4 mmol) was added dropwise into the 20 mL Schlenk tube containing 5 mL THF solution of complex **3** (0.073 g, 0.1 mmol) via cannula under positive N_2 pressure. After being stirred for 1 h, the reaction solution was dried under vacuum. The residue was redissolved in 5 mL THF under N_2 and then the THF solution was monitored by FTIR. The IR spectrum showing ν_{NO} stretching frequencies at 1760 (s), 1708 (s) cm^{-1} (THF) was assigned to the formation of the known complex [PPh_4][$(C_3H_3N_2)(PhS)Fe(NO)_2$] (**7**) [33]. The reaction mixture was filtered through Celite to separate the insoluble solid. The filtrate was concentrated under reduced pressure and then hexane was added to the filtrate to precipitate the brown solid **7** (yield 0.180 g, 71.1%).

2.10. EPR measurement

X-band EPR spectra were recorded on a Bruker EMX spectrometer equipped with a Bruker TE102 cavity. The microwave frequency was measured with a Hewlett–Packard 5246L electronic counter. At 298 K, X-band EPR spectrum of complex **1** in THF was obtained with a microwave power of 19.971 mW, frequency at 9.506 GHz, and modulation amplitude of 0.80 G at 100.00 kHz. At 77 K, the EPR spectrum of complex **1** frozen in THF was obtained with a microwave power of 19.971 mW, frequency at 9.506 GHz, and modulation amplitude of 1.6 G at 100 KHz.

2.11. Magnetic measurements

The magnetic data were recorded on a SQUID magnetometer (MPMS VSM by Quantum Design Company) under 0.5 T external magnetic field in the temperature range 4–300 K. The magnetic susceptibility data were corrected with temperature independent paramagnetism (TIP, 2×10^{-4} cm^3 mol^{-1}), and ligands' diamagnetism by the tabulated Pascal's constants.

2.12. Crystallography

Crystallographic data of complex **1** is summarized in Table 1. The crystals of **1** are blocks. The crystal was mounted on a glass fiber and quickly coated in epoxy resin. Unit-cell parameters were obtained by least-squares refinement. Diffraction measurements for complex **1** was carried out on a Nonius Kappa CCD diffractometer using graphite-monochromated Mo Kα radiation (λ = 0.7107 Å). Least-squares refinement of the positional and anisotropic thermal parameters for the contribution of all non-hydrogen atoms and fixed hydrogen atoms was based on F^2. A SADABS absorption correction was made. The SHELXTL structure refinement program was employed.

3. Results and discussion

3.1. Synthesis and characterization

As presented in Scheme 1a, the addition of 2 equiv. of TMEDA to a THF solution of $[Fe(\mu\text{-}I)(NO)_2]_2$ at ambient temperature caused an immediate color change from red-brown to yellow-green. The substantial amounts of neutral five-coordinate $\{Fe(NO)_2\}^9$ [(TMEDA)$Fe(NO)_2I$] (**1**) were isolated as dark brown solid after recrystallization from THF–hexane in 81% yield. Complex **1** is soluble in CH_2Cl_2, THF, and CH_3CN and displays moderately air sensitivity in solution. The IR spectrum of complex **1** exhibits two diagnostic ν_{NO} stretching frequencies at 1770 (s), 1715 (vs) cm^{-1} (THF), consistent with the presence of an $Fe(NO)_2$ moiety. At 298 K, the EPR spectrum of complex **1** displays a six-line spectrum with signal g = 2.031 and the hyperfine coupling constant a_I = 37.6 G. (Fig. 1a and c). The EPR signal g = 2.031 of complex **1** is identical to the characteristic g value of the protein-bound DNICs and low-molecular-weight DNICs in vitro/vivo [17]; however, it is different from

Table 1
Crystallographic data of complex **1**.

Chemical formula	$C_6H_{16}FeIN_4O_2$
Formula weight	358.98
Crystal system	Orthorhombic
Space group	*Cmc2(1)*
λ (Å) (Mo Kα)	0.71073
a (Å)	10.3160(4)
b (Å)	13.5816(5)
c (Å)	9.5035(3)
α (°)	90
β (°)	90
γ (°)	90
V (Å^3)	1331.51(8)
Z	4
d_{calc} (g cm^{-3})	1.791
μ (mm^{-1})	3.437
T (K)	295(2)
R	0.0274[a]
R^2_{WF}	0.0460[b]
Goodness-of-fit (GOF)	1.048

[a] $R = \sum |(F_o - F_c)| / \sum F_o$.

[b] $R^2_{WF} = \left\{ \sum w\left(F_o^2 - F_c^2\right)^2 / \sum \left[w\left(F_o^2\right)^2 \right] \right\}^{\frac{1}{2}}$.

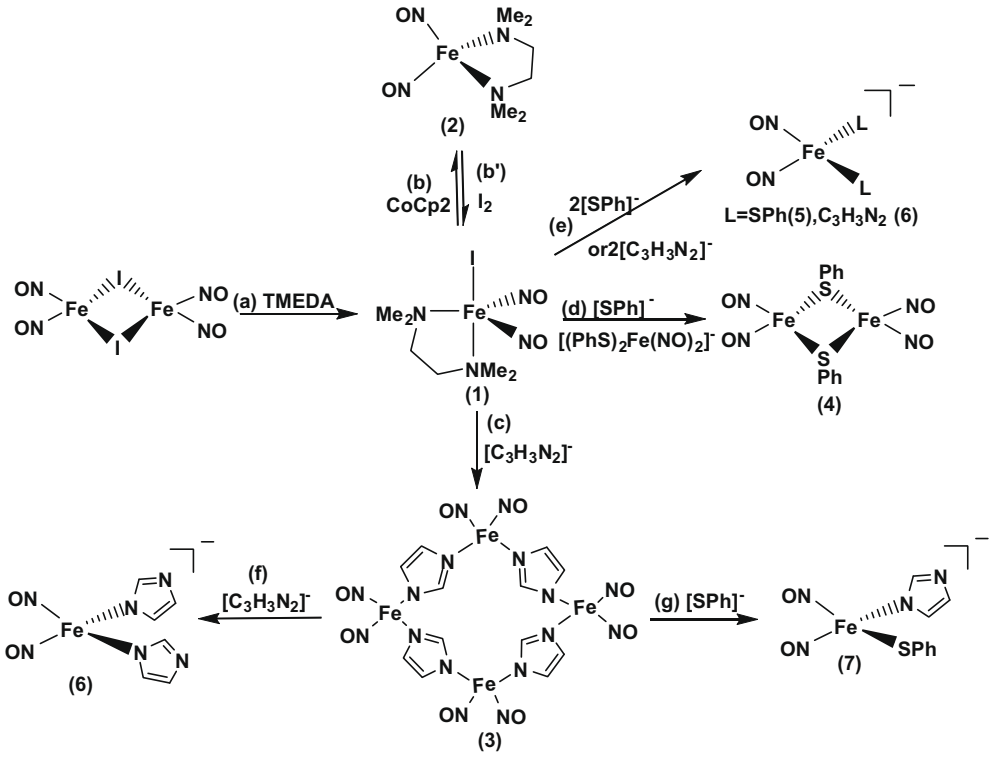

Scheme 1.

the g value of 2.01 for the six-coordinate DNICs [35]. The coincident g values of EPR among complex **1**, protein-bound DNICs and low-molecular-weight DNICs implicate the probable existence of five-coordinate DNICs in vitro/vivo. At 77 K, the EPR spectrum of complex **1** shows the rhombic signal with $g_1 = 2.10$, $g_2 = 2.03$, $g_3 = 1.97$ (Fig. 1b). Magnetic susceptibility data of a powder sample of complex **1** were collected in the temperature range of 4–300 K in 5 kG (0.5 T). The net molar magnetic susceptibility (χ_M) increased from 2.11×10^{-3} cm^3 mol^{-1} at 300 K to 0.055 cm^3 mol^{-1} at 4 K. The temperature-dependent effective magnetic moment (μ_{eff}) decreases from 2.248 μ_B at 300 K to 1.332 μ_B at 4 K (Fig. 2). The comparisons of complex **1** and the extremely unstable cationic four-coordinated $\{Fe(NO)_2\}^9$ $[(TMEDA)Fe(NO)_2]^+$ implies that the fifth ligand, iodide of complex **1** appropriately makes up the electronic deficiency of $[(TMEDA)Fe(NO)_2]^+$ to stabilize the $\{Fe(NO)_2\}^9$ moiety [31]. The observation is consistent with another stable five-coordinate $\{Fe(NO)_2\}^9$ $[(6\text{-}Me_3\text{-}TPA)Fe(NO)_2][ClO_4]$ in which the three N atoms of amine and pyridines were ligated to the $\{Fe(NO)_2\}^9$ moiety [36].

3.2. Reactivity

The reversible interconversion between the five-coordinate $\{Fe(NO)_2\}^9$ complex **1** and four-coordinated $\{Fe(NO)_2\}^{10}$ [(TMEDA)$Fe(NO)_2$] (**2**) was monitored by IR ν_{NO} spectra (Scheme 1b and b′). As shown in Scheme 1b, addition of one equiv of $CoCp_2$ into the THF solution of complex **1** resulted in the color change from yellow-green to green. The shift of NO stretching frequencies from 1770 (s), 1715 (s) to 1698 (s), 1644 (s) cm^{-1} was assigned to the formation of the well-known neutral $\{Fe(NO)_2\}^{10}$ complex **2** [31]. Reversibly, when the THF solution of I_2 was added to 2 equiv. of complex **2** in THF drop by drop, the shift of NO stretching frequencies from 1698 (s), 1644 (s) to 1770 (s), 1715 (s) cm^{-1} indicated the reformation of complex **1**, presumably, via the oxidative addition of I_2 to 2 equiv. of the neutral $\{Fe(NO)_2\}^{10}$ complex **2** (Scheme 1b′). The interconversion between complexes **1** and **2** shows that the coordinated iodo ligand of complex **1** reimburses the electronic deficiency of the $\{Fe(NO)_2\}^9$ core containing [amine, amine] ligation mode to stabilize complex **1**. In addition, the reduction of the electron deficient $\{Fe(NO)_2\}^9$ core of complex **1** to the electron rich $\{Fe(NO)_2\}^{10}$ core results in the dissociation of iodo ligand of complex **1** and yields the stable four-coordinate complex **2**, since the cationic $\{Fe(NO)_2\}^9$ $[(sparteine)Fe(NO)_2]^+$ was reported as a thermally unstable species.

Interestingly, when 1 equiv of complex **1** was added to the CH_3CN solution of $[Na\text{-}18\text{-}crown\text{-}6\text{-}ether][C_3H_3N_2]$ at ambient temperature, the known tetramer $[Fe(NO)_2(C_3H_3N_2)]_4$ (**3**) [25], characterized by IR, UV–vis, EPR, and single-crystal X-ray diffraction, was precipitated as light brown solid (Scheme 1c). Similarly, reaction of complex **1** with 1 equiv. of $[PPh_4][SPh]$ resulted in the Roussin's red ester $[Fe(\mu\text{-}SPh)(NO)_2]_2$ (**4**) identified by the IR ν_{NO} stretching frequencies (1814 (w), 1783 (s), 1756 (s) cm^{-1} (THF)) (Scheme 1d) [38]. A reasonable reaction sequence was proposed to account for the formation of complexes **3** and **4**. The substitution of weak electron donating ligand I^- with the stronger donating ligands $[SPh]^-$ and $[C_3H_3N_2]^-$ yielded the intermediates [(TMEDA)$Fe(NO)_2(SPh)$] and [(TMEDA)$Fe(NO)_2(C_3H_3N_2)$], respectively. The electronic richer Fe centers of the intermediates triggered the dissociation of TMEDA from the intermediate and subsequently transformed to the stable complexes **3** and **4**. Upon the addition of 4 equiv. of $[Na][C_3H_3N_2]$ and 18-crown-6-ether to the THF solution of complex **3**, the reaction monitored by the shift of IR ν_{NO} stretching frequencies from 1800 (s), 1736 (s) to 1774 (s), 1712 (s) cm^{-1} implied the formation of [Na-18-crown-6-ether]-$[Fe(NO)_2(C_3H_3N_2)_2]$ (**6**) with two imidazolates (Scheme 1f). In a similar fashion, reaction of 4 equiv of $[PPh_4][SPh]$ with complex **3** afforded $[PPh_4][Fe(NO)_2(C_3H_3N_2)(SPh)]$ (**7**) with the mixed thiolate-imidazolate ligands, identified by IR, UV–vis and EPR (Scheme 1g) [33]. Alternatively, the nucleophilic attack of $[C_3H_3N_2]^-$ to Roussin's red ester $[Fe(\mu\text{-}SPh)(NO)_2]_2$ (**4**) led to the formation of

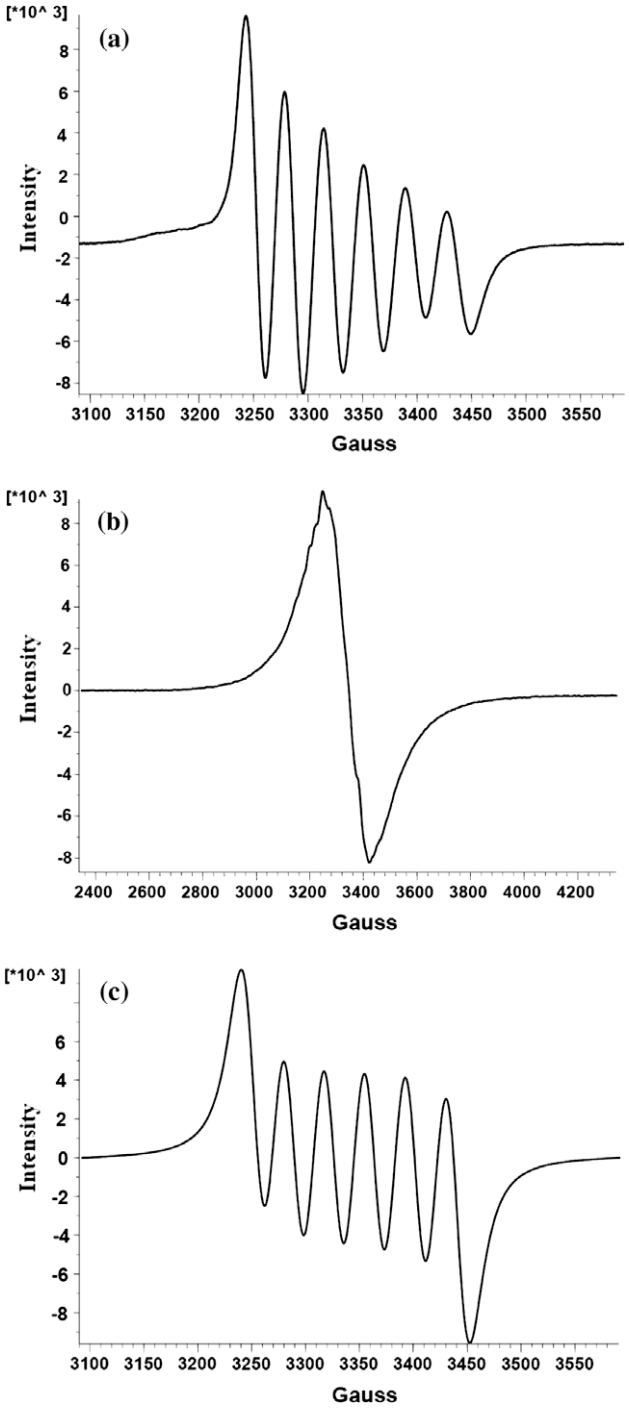

Fig. 1. EPR spectra of complex **1** (a) at 298 K (g = 2.031); (b) at 77 K (g_x = 2.10, g_y = 2.03, and g_z = 1.97); and (c) the simulated EPR spectrum of complex **1** with hyperfine coupling constant of a_1 = 37.6 G.

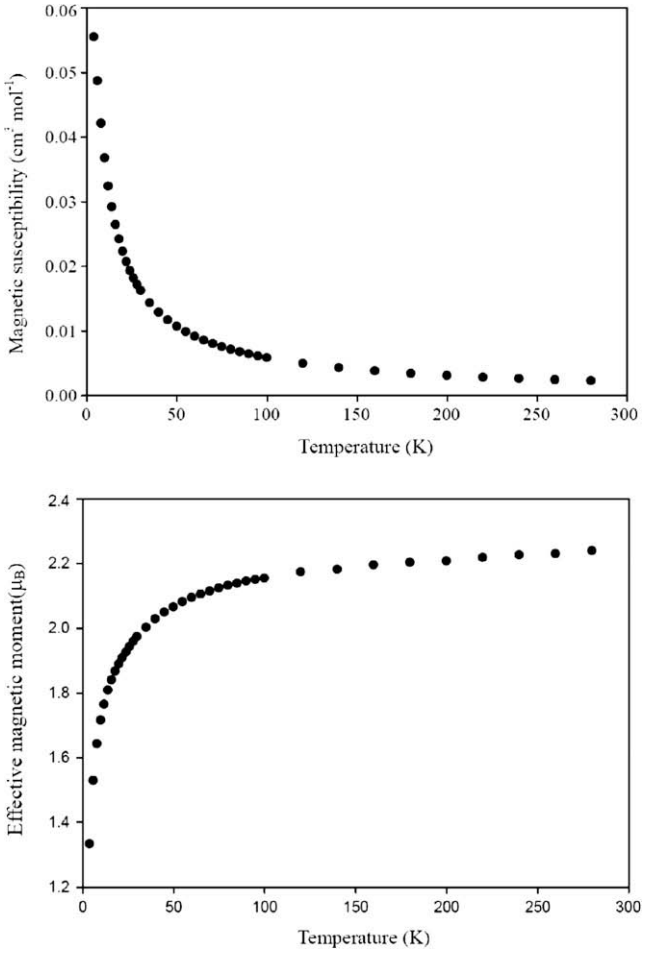

Fig. 2. Plots of molar magnetic susceptibility (top) and effective magnetic moment (bottom) versus temperature for complex **1**.

complex **7** via the bridged-thiolate cleavage [33]. These results show that the cyclic tetra-nuclear complex **3** and dinuclear complex **4** could serve as the precursor for the syntheses of the other DNICs containing imidazolate or thiolate ligand via the nucleophilic attack pathway. As shown in Scheme 1d, the reaction of complex **1** with complex **5** resulted in the shift in ν_{NO} from 1770 (s), 1715 (s) cm^{-1} (**1**) to 1814 (w), 1783 (s), 1756 (s) cm^{-1} (THF) which was in accordance with the formation of complex **4** (Scheme 1d) and indicated that complex **1** behaved as the reagent of $\{Fe(NO)_2\}^9$ moiety. Complexes **5** and **6** were obtained from the reaction of complex **1** with 2 equiv. of $[PPh_4][SPh]$ and [Na-18-crown-6-ether][$C_3H_3N_2$], respectively (Scheme 1e). The reactions also demonstrated that complex **1** possessed the character as the donor $\{Fe(NO)_2\}^9$ moiety. In contrast to the unstable $\{Fe(NO)_2\}^9$ $[(sparteine)Fe(NO)_2]^+$, complex **1** could act as a stable donor reagent of $\{Fe(NO)_2\}^9$ moiety for the syntheses of other DNICs .

3.3. Structure

The crystal structure of complex **1** is shown in Fig. 3 and selected bond distances and angles are given in the figure captions. The geometry of iron center of complex **1** is best described as a distorted trigonal bipyramidal with two nitrosyl groups positioned in the equatorial plane. The two NO ligands are equivalent crystallographically and the $Fe(NO)_2$ unit in the complex is almost planar. The strain effect of the chelating ligand generates a 80.7(2)° N(2)–Fe–N(3) angle, enforcing distortion from trigonal bipyramidal at the five-coordinate Fe site in complex **1**. The observation that the N(1A)–Fe–N(1) angle of 113.1° is larger than the O(1A)–Fe–O(1) angle of 99.07° indicates that the iron-dinitrosyl group is an "attracto" conformation whose N–M–N bond angle is less than 130° and two oxygen atoms bend toward each other. The "attracto" conformations are generally observed for the first-low transition-metal complexes coordinated with good π-acceptor ligands [39,40]. The Fe–N(1) bond length of 1.673(4) Å falls in the range from 1.661(4) to 1.695(3) Å for the anion/neutral/cationic $\{Fe(NO)_2\}^9$ DNICs. Moreover, the N(1)–O(1) bond length of

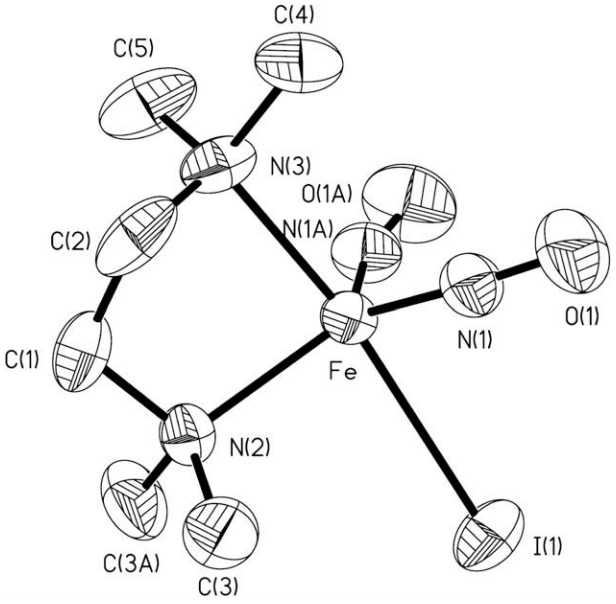

Fig. 3. ORTEP drawing and labeling scheme of [(TMEDA)Fe(NO)$_2$I] with thermal ellipsoids drawn at 30% probability. Hydrogen atoms are omitted for clarity. Selected bond distances (Å) and angles (°): Fe–N(1) 1.673(4); Fe–N(2) 2.146(5); Fe–N(3) 2.238(8); Fe–I(1) 2.8867(10); N(3)–Fe–I(1) 172.47(18); N(1)–O(1) 1.169(5); N(1A)–Fe–N(1) 113.1(3); N(1A)–Fe–N(2) 123.45(15); N(1)–Fe–N(2) 123.45(15); N(2)–Fe–N(3) 80.7(2); N(2)–Fe–I(1) 91.81(17); N(1)–Fe–N(3) 95.57(18); N(1)–Fe–I(1) 88.56(15); and O(1)–N(1)–Fe 162.6(5).

1.169(5) Å also falls in the range from 1.160(6) to 1.178(3) Å for the anion/neutral/cationic {Fe(NO)$_2$}^{9} DNICs [31].

4. Conclusions

Studies on the neutral five-coordinate {Fe(NO)$_2$}^{9} [(TMEDA)Fe(NO)$_2$I] (**1**) have resulted in the following conclusions:

(1) The neutral five-coordinate complex **1** was synthesized by the reaction of [Fe(μ-I)(NO)$_2$]$_2$ with TMEDA under mild conditions and characterized by UV–vis, IR, and single-crystal X-ray diffraction. The EPR signal g = 2.031 of complex **1** is consistent with the characteristic g value of four-coordinate DNICs and implies the probably existence of the five-coordinate DNIC in vivo/vitro.
(2) The reversible interconversion between the five-coordinate {Fe(NO)$_2$}^{9} complex **1** and the four-coordinate {Fe(NO)$_2$}^{10} complex **2** reveals that the {Fe(NO)$_2$}^{10} DNICs with [amine, amine] ligation mode favor the four-ligation coordination sphere, in contrast, the {Fe(NO)$_2$}^{9} DNICs with [amine, amine] ligation mode favors the ligation of the fifth weak donating ligand (I^-) to the Fe center to stabilize complex **1**.
(3) The facile transformation of the neutral complex **1** to complexes **3**, **4**, 5 and **6** reveals that complex **1** acts as an {Fe(NO)$_2$}^{9}-donor reagent in the presence of thiolates or imidazolates.
(4) For the synthetic methodology, complex **1** serves as a precursor for the syntheses of biomimetic DNICs containing the various ligation modes ([N,N]/ [N,S]/[S,S]).

Acknowledgement

We gratefully acknowledge financial support from the National Science Council (Taiwan).

Appendix A. Supplementary material

Supplementary data associated with this article can be found, in the online version, at doi:10.1016/j.jorganchem.2009.06.040.

References

[1] F.T. Bonner, G. Stedman, The chemistry of nitric oxide and redox-related species, in: M. Feelisch, J.S. Stamler (Eds.), Methods in Nitric Oxide Research, John Wiley & Sons Ltd., New York, 1996, pp. 3–18.
[2] E.A. Jaimes, J. Am. Soc. Nephrol. 12 (2001) 1204–1210.
[3] G.C. May, Brit. J. Pharmacol. 102 (1991) 759–763.
[4] Y.P. Tao, T.P. Misko, A.C. Howlette, C. Klein, Development 124 (1997) 3587–3595.
[5] J. MacMicking, Q. Xie, C. Nathan, Annu. Rev. Immunol. 15 (1997) 323–350.
[6] J.A. McCleverty, Chem. Rev. 104 (2004) 403–418.
[7] C. Badorff, B. Fichtlscherer, A. Muelsch, A.M. Zeiher, S. Dimmeler, Nitric Oxide 6 (2002) 305–312.
[8] J.S. Stamler, D.J. Singel, J. Loscalzo, Science 258 (1992) 1898–1902.
[9] J.S. Stamler, Cell 78 (1994) 931–936.
[10] F.A.C. Wiegant, I.Y. Malyshev, A.L. Kleschyov, E. Van Faassend, A.F. Vanin, FEBS Lett. 455 (1999) 179–182.
[11] M. Boese, P.I. Mordvintcev, A.F. Vanin, R. Busse, A. Muelsch, J. Biol. Chem. 270 (1995) 29244–29249.
[12] A. Mulsch, P. Mordvintcev, A.F. Vanin, R. Busse, FEBS Lett. 294 (1991) 252–256.
[13] Y. Henry, M. Lepoivre, J.C. Drapier, C. Ducrocq, J.L. Boucher, A. Guissani, FASEB J. 7 (1993) 1124–1134.
[14] A.J. Vithayathil, J.L. Ternberg, B. Commoner, Nature 207 (1965) 1246–1249.
[15] M.W. Foster, J.A. Cowan, J. Am. Chem. Soc. 121 (1999) 4093–4100.
[16] C.E. Cooper, Biochim. Biophys. Acta, Bioenergy 1411 (1999) 290–309.
[17] A.R. Butler, I.L. Megson, Chem. Rev. 102 (2002) 1155–1165.
[18] H. Lewandowska, S. Meczynska, B. Sochanowicz, J. Sadlo, M. Kruszewski, J. Biol. Inorg. Chem. 12 (2007) 345–352.
[19] H. Ding, Proc. Natl. Acad. Sci. USA 97 (2000) 5146–5150.
[20] P. Turella, J.Z. Pedersen, A.M. Caccuri, F. De Maria, P. Mastroberardino, J. Biol. Chem. 278 (2003) 42294–42299.
[21] E. Cesareo, L.J. Parker, J.Z. Pedersen, M. Nuccetelli, A.P. Mazzetti, A. Pastore, G. Federici, A.M. Caccuri, G. Ricci, J.J. Adams, M.W. Parker, M. Lo Vanin, J. Biol. Chem. 280 (2005) 42172–42180.
[22] J.R. Lancaster Jr., J.B. Hibbs, Proc. Natl. Acad. Sci. USA 87 (1990) 1223–1227.
[23] M. Lee, P. Arosio, A. Cozzi, N.D. Chasteen, Biochemistry 33 (1994) 3679–3687.
[24] B. D'Autreaux, O. Horner, J.-L. Oddou, C. Jeandey, S. Gambarelli, C. Berthomieu, J.-M. Latour, I. Michaud-Soret, J. Am. Chem. Soc. 126 (2004) 6005–6016.
[25] C. Badorff, B. Fichtlscherer, A. Muelsch, A.M. Zeiher, S. Dimmeler, Nitric Oxide 6 (2002) 305–312.
[26] N. Reginato, C.T.C. McCrory, D. Pervitsky, L. Li, J. Am. Chem. Soc. 121 (1999) 10217–10218.
[27] M.-L. Tsai, C.-C. Chen, I.J. Hsu, S.-C. Ke, C.-H. Hsieh, K.-A. Chiang, G.-H. Lee, Y. Wang, J.-M. Chen, J.-F. Lee, W.-F. Liaw, Inorg. Chem. 43 (2004) 5159–5167.
[28] F.-T. Tsai, S.-J. Chiou, M.-C. Tsai, M.-L. Tsai, H.-W. Huang, M.-H. Chiang, W.-F. Liaw, Inorg. Chem. 44 (2005) 5872–5881.
[29] T.-T. Lu, S.-J. Chiou, C.-Y. Chen, W.-F. Liaw, Inorg. Chem. 45 (2006) 8799–8806.
[30] M.-L. Tsai, W.-F. Liaw, Inorg. Chem. 45 (2006) 6583–6585.
[31] M.-C. Hung, M.-C. Tsai, G.-H. Lee, W.-F. Liaw, Inorg. Chem. 45 (2006) 6041–6047.
[32] M.-L. Tsai, C.-H. Hsieh, W.-F. Liaw, Inorg. Chem. 46 (2007) 5110–5117.
[33] H.-W. Huang, C.-C. Tsou, T.-S. Kuo, W.-F. Liaw, Inorg. Chem. 47 (2008) 2196–2204.
[34] S.-J. Chiou, C.-C. Wang, C.-M. Chang, J. Organomet. Chem. 693 (2008) 3582–3586.
[35] F.-T. Tsai, T.-S. Kuo, W.-F. Liaw, J. Am. Chem. Soc. 131 (2009) 3426–3427.
[36] D.-H. Jo, Y.-M. Chiou, L. Que Jr., Inorg. Chem. 40 (2001) 3181–3190.
[37] B. Haymore, R.D. Feltham, Inorg. Synth. 14 (1973) 82–86.
[38] T.B. Rauchfuss, T.D. Weatherill, Inorg. Chem. 21 (1982) 827–830.
[39] J.H. Enemark, R.D. Feltham, Coord. Chem. Rev. 13 (1974) 339–406.
[40] G.B. Richter-Addo, P. Legzdins, Metal Nitrosyls, Oxford University Press, New York, 1992. p. 81.